Original Article

DOI: 10.5582/bst.2012.v6.5.262

Effects of Xiaoqinglong decoction on gene expression profiles in a rat chronic obstructive pulmonary disease model

Caiqing Zhang[1,#], Lili Feng[2,#], Ming Li[3,*], Chongjuan Dong[4], Wei Zhang[5,*]

[1] *Department of Respiratory Medicine, Qianfoshan Hospital Affiliated to Shandong University, Ji'nan, China;*
[2] *Department of Hematology, Provincial Hospital Affiliated to Shandong University, Ji'nan, China;*
[3] *Department of Rheumatology and Clinical Immunology, Provincial Hospital Affiliated to Shandong University, Ji'nan, China;*
[4] *Department of Pediatrics, Wendeng Central Hospital of Weihai City Affiliated to Weifang Medical College, Wendeng, China;*
[5] *Department of Respiratory, the First Affiliated Hospital of Shandong University of Traditional Chinese Medicine, Ji'nan, China.*

Summary **Xiaoqinglong decoction (XQLD) has been used for centuries in Asia to effectively treat patients with chronic obstructive pulmonary disease (COPD). However, its mechanisms remain unknown. To elucidate this problem, we analyzed the effects of XQLD on gene expressions profiles in COPD rats. In the study, 20 male Wistar rats were injected with lipopolysaccharide (LPS), exposed to cigarette smoke and kept at −20°C for 5 min/day for a successive 8 days to establish COPD animals. Trachea ultramicrostructure and histomorphology were observed to determine whether these models were established successfully. Gene expression profiles were detected using cDNA microarrays. We found 56 differentially expressed genes associated with COPD progression, including 32 up-regulated genes and 24 down-regulated genes. These genes were confirmed to be involved in immune and inflammation reactions, metabolism, cell transportation and the cell cycle, signal transduction and gene regulation. Comparison of gene expression between the therapy group and control group showed that there were only 11 differentially expressed genes, including 5 up-regulated genes and 6 down-regulated genes. We concluded that XQLD had therapeutic effects in COPD rats by affecting gene expression. Pharmacological or targeted expression of some genes might be found useful as novel therapy in COPD management.**

Keywords: Pulmonary disease, chronic obstructive, Xiaoqinglong decoction (XQLD), cDNA microarrays

1. Introduction

Chronic obstructive pulmonary disease (COPD) is the fourth most common global cause of death and also exerts an enormous toll on patient quality of life (*1*). Currently, treatment of COPD is suboptimal. In the past, long-term administration of antibiotics was used to treat acute exacerbations of COPD, but meta-analyses of the studies of antibiotic administration showed no significant benefit (*2*). A multicenter, cross-sectional, observational study was conducted in 30 Spanish hospitals among COPD patients aged > 40 years who were hospitalized for an acute exacerbation showed that antibiotic use was significantly associated with yellow or green-yellow sputum prior to the exacerbation, a higher number of exacerbations in the previous year, more visits to emergency departments, and bronchiectasis (*3*). Because of these problems with antibiotic treatment, more and more traditional Chinese physicians are focusing on exploring the therapeutic effect of Chinese herbal medicine in COPD.

Xiaoqinglong decoction (XQLD) was from Shan

[#]*Co-first author:* These two authors contributed equally to this work.
**Address correspondence to:*
Dr. Ming Li, Department of Rheumatology and Clinical Immunology, Provincial Hospital Affiliated to Shandong University, No. 324 Jingwu Weiqi Road, Ji'nan, 250021, China.
E-mail: simlas2006@yahoo.com.cn
Dr. Wei Zhang, Department of Respiratory, the First Affiliated Hospital of Shandong University of Traditional Chinese Medicine, Ji'nan, 250021, China.
E-mail: wmx1104@163.com

Han Lun, a famous formulary in traditional Chinese medicine (*4*). The components of XQLD included Ma Huang (9 g), Gui Zhi (6 g), Bai Shao (9 g), Gan Jiang (3 g), Xi Xin (3 g), Zhi Gan Cao (6 g), Ban Xia (9 g) and Wu Wei Zi (3 g) and its major active constituents were ephedrine, cinnamic acid, peoniflorin, methyleugenol, glycyrrhizin and schisandrin. XQLD has been used for asthma, chronic bronchitis, allergic rhinitis, pneumonia, COPD, and sick sinus syndrome therapy for many years. The therapeutic effect of XQLD in COPD patients has received most traditional Chinese physicians' approval. Its side effects are fewer than antibiotics and it will not generate resistance as antibiotics do. Based on these advantages, the usage of XQLD in COPD treatment and related mechanisms have acquired wide attention recently. Its functional mechanism may be related to multiple factors (*5*). It was reported that XQLD could inhibit inflammatory cytokines, including IL-4, IL-8, TNF-α, and IFN-γ (*6*), rectify imbalance of oxidation/anti-oxidation and alleviate inflammatory reactions in COPD rats (*4*). And also, it could ameliorate pathological changes of airway inflammation and remodeling in COPD models. We have also documented that XQLD treatment could significantly lower expression of γ-glutamylcysteine synthetase and nuclear factor-κB in bronchial and alveolar epithelium of COPD rats (*4*). However, the precise molecular and genetic mechanism of XQLD in COPD therapy remains to be determined.

Gene expression profiles of diseased tissues help us to provide insight into the molecular mechanisms of disease and may eventually lead to the identification of novel therapeutic targets. Gene expression profileanalysis has been used in many diseases, including respiratory system diseases, such as acute lung injury (*7*). In the current study, to evaluate the effect of XQLD on COPD, we established a modified rat COPD model following previous studies described by Nie YC *et al.* (*8*), Song YP *et al.* (*9*), and Sun GR *et al.* (*10*). Differentially expressed genes were screened by a cDNA microarray technique after COPD rats were established to explore effects of XQLD on gene expression profiles. The relationship between alteration of gene expression and disease progress in rats helped us to elucidate the pathogeneses of COPD, understand the mechanisms of XQLD in COPD therapy and explore new potential novel therapeutic targets in COPD.

2. Materials and Methods

2.1. *Animals and reagents*

Thirty 2-month-old male Wistar rats were purchased from the Center of Medical Experimental Animals of Shandong University (Grade SPF, Certificated SCXK Lu2003004) (Ji'nan, China) and maintained in accordance with guidelines of the committee on Care and Use of Laboratory Animals of the Institute of Laboratory Resources, National Research Council (DHEW publication No. [NIH] FS-23) on Animal Care. Animals were divided into 3 experimental groups at random. Twenty rats were used to induce COPD models. Ten animals with this disease received XQLD therapy (therapy group) and the other ten were treated with PBS (model group). Ten normal Wistar rats were used as controls (control group). LPS was obtained from Sigma (St. Louis, MO, USA). Pentobarbital sodium was purchased from China National Medicine Group Shanghai Chemical Reagent Company. Reagents for XQLD were purchased from the pharmacy of Shandong University of Traditional Chinese Medicine. All the herbs were decocted with water and the final concentration was 0.6 g/mL. Sterilization of this decoction was carried out by steam sterilizer.

2.2. *Experimental procedures*

We established a modified rat COPD model following previous studies (*8-10*) and the treatment schema is shown in Figure 1. At first, a normal rat COPD model was established with LPS injection and cigarette smoke (CS) which has been documented to be a reliable COPD model (*8*). LPS was injected into rats through the trachea after they were anesthetized with 0.4% pentobarbital sodium (50 mg/kg) at day 1 and day 14. Animals were fixed and their glottises were exposed. An intravenous cannula was inserted into the trachea quickly and its plunger was drawn out. Then it was connected with another syringe. At the zero point two mL (200 μg) LPS, dissolved in normal saline, was pushed into the trachea. Rats were erected immediately and swiveled to distribute LPS in the lungs. CS was given twice a day from day 2 to day 28 (except day 1 and day 14). Nine point zero three grams of a cigarette was burned and CS lasted for 1 h each time. The second CS was given after 4 h. The normal rat COPD model was then modified by keeping rats at −20°C for 5 min/day from day 22 to day 29 according to the methods described by Sun GR *et al.* (*10*). Sun GR *et al.* found that there were more inflammatory cell infiltration in the modified rat COPD model than that in the normal rat COPD model from pathological characteristics analysis. Subsequently, rats in the therapy group were drenched with 2 mL XLQD (total dose = 7.5 × clinical dose in adult) from day 30 to day 43 (*4*). Rats in the model group were treated with PBS and rats in the control group were held under the same conditions without any intervention.

2.3. *Observation of trachea ultramicrostructure*

At day 44, all animals were sacrificed. 1-1.5 cm upper eminence trachea tissues were collected, and fixed with

2% glutaraldehyde for 2 h at 4°C. After washing with PBS, they were fixed for 1 h with osmium tetroxide at 4°C and then washed twice with double distilled water. Following dehydration with alcohol, they were dried. At last, samples were stuck to a metal sample table with paste which can conduct electricity, covered by a metal membrane and then observed using scanning electron microscopy.

2.4. *Histomorphology performances under light microscope*

Paraffin-embedded sections of lung tissue were de-paraffinized in xylene and ethanol, stained with hematoxylin-esoin (H&E) and observed under a light microscope (Nikon Corporation, Tokyo, Japan). Trachea pathology grade was judged according to a modified criterion designed by Barbera *et al.* (*11*) (Table 1).

2.5. *General appearances observation and body mass growth index calculation*

Animal general appearances were observed during the whole process, which included animal movement, fur appearance, weight growth, respiration situation and cough severity. Animal body mass growth index was calculated as follows: Body mass growth index = (body mass before experiment – body mass after experiment) /body mass before experiment.

2.6. *Total RNA extraction and cDNA microarray screening*

Lung tissues were selected randomly from each group and total RNA was extracted with Trizol (Invitrogen, Carlsbad, CA, USA). RNA was purified with the NucleoSpin RNA clean-up kit (Macherey-Nagel, Düren, Germany). RNA optical density at 260 nm/280 nm was consistently > 1.8. RNA samples were reverse transcribed into single-strand cDNA, synthesized into double-strand cDNA, and transcribed into cRNA *in vitro* using the T7RiboMAX Express Large Scale RNA Production System (Promega, Madison, WI, USA). After reverse transcription with random primers, cRNA products were marked with the Klenow enzyme.

Samples were hybridized using a hybridization solution (25% formamide, 3× standard saline citrate [SSC], 0.2% sodium dodecyl sulfate [SDS], 5× Denhart's) at 42°C overnight in a humid environment. Subsequently, slides were washed with washing solution I (2× SSC, 0.2% SDS) at 42°C for 4 min, followed by washing solution II (2× SSC). Arrays were scanned using CapitalBio's confocal scanner LuxScan 10K-A (Beijing, China). An intensity-dependent lowess program in the R language package was used to normalize two channel ratio values. Statistical data and differential analysis files were generated by SAM software 3.0 (Stanford University, Stanford, CA, USA).

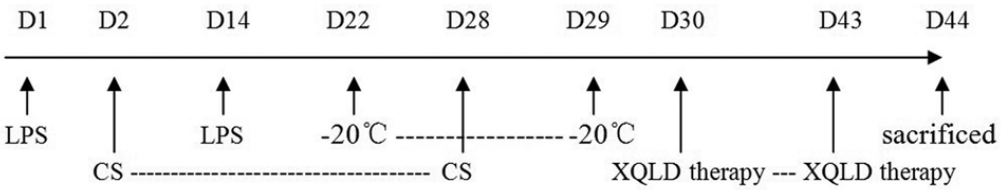

Figure 1. Schema of treatment. LPS (200 μg) was injected into rats through trachea at day 1 and day 14. CS was given twice per day from day 2 to day 28 (except day 14). Animals were kept at −20°C for 5 min/day from day 22 to day 29. Rats received 2 mL of XQLD therapy daily (0.6 g/mL) from day 30 to day 43. All the animals were sacrificed at day 44.

Table 1. Criterion of trachea pathology alteration grades

Histology appearances under microscope	Grade			
	0	1	2	3
Cilia lodging, adhesion and depletion	No	< 1/4 circle	1/4-1/2circle	> 1/2circle
Epithelial cell degeneration, necrosis and desquamate	No	< 1/4 circle	1/4-1/2 circle	> 1/2 circle
Beaker cell proliferation	No	< 1/4 circle	1/4-1/2 circle	> 1/2 circle
Epitheliial squamous metaplasia	No	< 1/4 circle	1/4-1/2 circle	> 1/2 circle
Mucous hyperemia and swelling	No	< 1/4 circle	1/4-1/2 circle	> 1/2 circle
Lymphocyte infiltration	No	Lymphoctes can be seen	Follicle can be seen	> 5 follicles
Mononuclear macrophage infiltration	No	< 10 /HP	10-20/HP	> 20/HP
Neutrophil infiltration	No	< 10/HP	10-20/HP	> 20/HP
Eosinophilic cell infiltration	No	< 10/HP	10-20/HP	> 20/HP
Smooth muscle cell breakage/hyperplasia	No	< 1/4 circle	1/4-1/2 circle	> 1/2 circle

Abreviations: HP, high power microscope.

2.7. *Statistical analysis*

SPSS 15.0 for Windows was used for all analyses. All data are expressed as mean ± standard deviation (mean ± S.D.). One-factor ANOVA was used for measurement data comparison of every group and a *q*-test was used for comparison of two groups. Comparisons of numerical data among groups were performed by χ^2 test. Difference between mean values is judged to be statistically significant when $p < 0.05$.

3. Results

3.1. *Trachea morphology and pathology appearances under scanning electron microscope and light microscope*

The scanning electron microscope showed that trachea cilia in the control group were uniform and in the same direction. However, there were lodging, adhesion and depletion with large amounts of secretion in the model group. Compared to the model group, the XQLD therapy group was obviously improved (Figure 2A).

We selected bronchioles (diameter: 700-1,200 μm) and lumen (the shortest diameter/the longest diameter ≥ 0.7) to analyze inflammation responses and small airway modeling. Histomorphology observations under the light microscope in the three groups are shown in Table 2 and Figure 2B. There were severe inflammatory responses in the model group and increased lymphocytes, monocytes and neutrophils can be seen in lung tissues. This phenomenon was accompanied by cilia lodging, adhesion and depletion, epithelial cell degeneration, necrosis and desquamate, goblet cell proliferation, epithelial squamous metaplasia, mucous hyperemia and swelling. These pathological changes confirmed that our COPD models were established successfully. After XQLD therapy, inflammatory responses were obviously relieved and the numbers of inflammatory cells, including lymphocytes, monocytes, and neutrophils, decreased significantly. Meanwhile, pathological changes of cilia, epithelial cells, goblet cells, epithelium and mucous membranes were dramatically relieved.

3.2. *General appearances*

Rats in the control group were active and restless, with

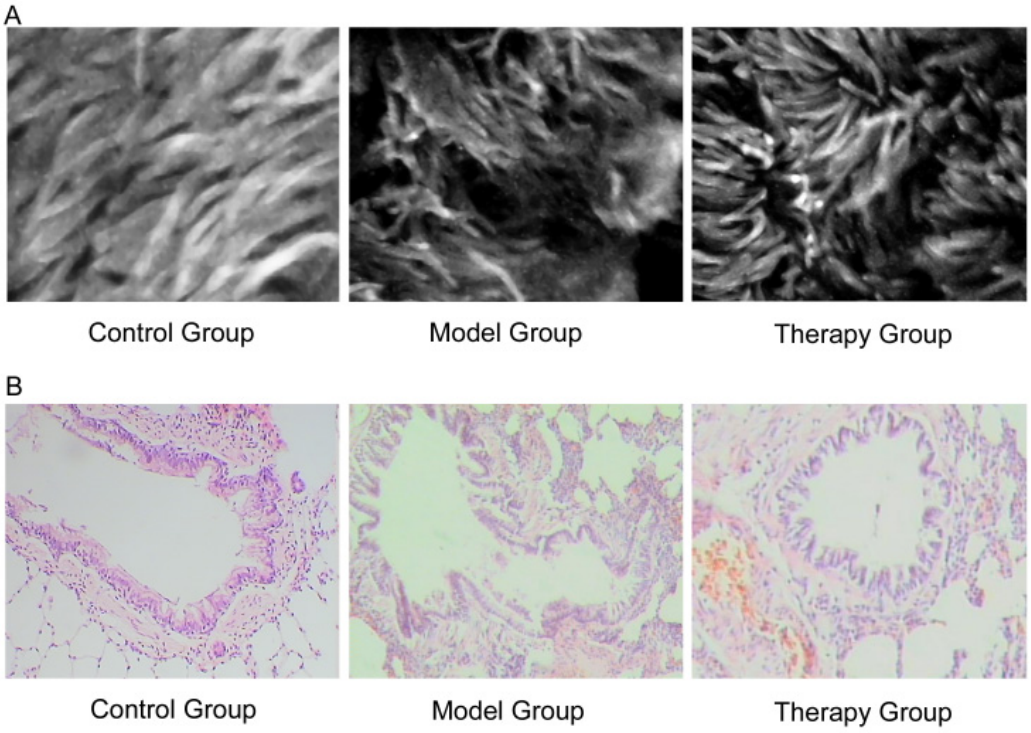

Figure 2. Trachea morphology and pathology appearances under scanning electron microscope and light microscope. Control group, Wistar rats without any treatment; Model group, rat COPD models treated with PBS; Therapy group, rat COPD models received Xiaoqinglong decoction therapy. (A) Alteration of trachea ultramicrostructure. Trachea tissues were collected and observed under scanning electron microscope. Control group (left, magnification ×6,000): Trachea cilia were uniform with same direction. Model group (middle, magnification ×6,000): Trachea cilia diminished dramatically. Depletion and large amounts of secretion can be seen. Therapy group (right, magnification ×6,000): After XQLD therapy, trachea cilia increased in a consistent direction and the secretions were obviously decreased. (B) Pathology appearance of trachea. Control group (left, magnification ×100): Epithelium of bronchiole was smooth and there was no inflammation cell infiltration, no hyperemia or no swelling. Model group (middle, magnification ×100): Bronchial lumen expansion, cilia adhesion and desquamated, goblet cell proliferation, surrounding blood capillary fibrosis hyperplasia were severe. More inflammatory cell infiltration could be found. Therapy group (right, magnification ×100): Inflammation around trachea lessened after XQLD therapy. The number of inflammatory cells decreased dramatically.

Table 2. Inflammation responses and small airway reconstitutions in indicated groups

Histology appearances under microscope	Grade		
	Model group	Therapy group	Control group
Cilia lodging, adhesion and depletion	2-3	1-2	0
Epithelial cell degeneration, necrosis and desquamate	2-3	1-2	0-1
Beaker cell proliferation	1-3	1-2	0
Epithelial squamous metaplasia	2-3	1-2	0
Mucous hyperemia and swelling	1-3	1-2	0
Lymphocyte infiltration	2-3	1-3	0-1
Mononuclear macrophage infiltration	1	1	0-1
Neutrophil infiltration	1-2	1-2	0-1
Eosinophilic cell infiltration	1	1	0
Smooth muscle cell breakage/hyperplasia	1-3	1-2	0

Model group, rat COPD models treated with PBS; Therapy group, rat COPD models received Xiaoqinglong decoction therapy; Control group, Wistar rats without any treatment.

smooth and burnished fur. Their body mass increased gradually and respiration was stable. Before XQLD therapy, rats in the model group and therapy group usually stayed still, extradoed and wriggled with gathered fur. Their body mass increased slowly and respiration was short accompanied by frequent cough. Cough appeared at the first day of CS and lasted to the end of our experiment. At day 28, rats in the model group and therapy group appeared to have shortness of breath. These symptoms of rats in the therapy group were obviously alleviated after XQLD therapy. Body mass growth indexes in the three groups are shown in Figure 3.

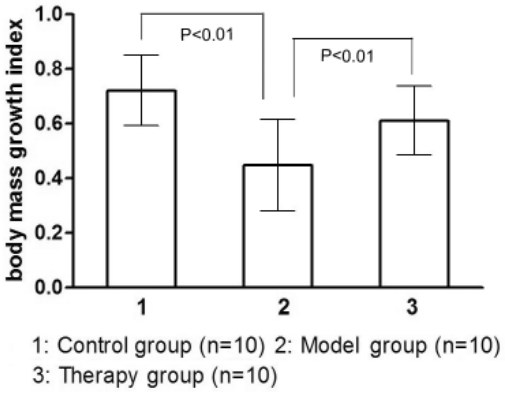

Figure 3. Body mass growth index in three groups. Control group, Wistar rats without any treatment; Model group, rat COPD models treated with PBS; Therapy group, rat COPD models received Xiaoqinglong decoction therapy. Rat body mass growth indexes in indicated groups were measured. It was obviously lower in model group and therapy group than that in the control group. Compared with model group, rat weight growth index increased significantly after XQLD therapy ($p < 0.01$).

3.3. *Analysis of gene expression profiles*

Genes were judged to be differentially expressed genes when the mean value exceeded 2.5 or lower than 0.375 to increase research reliability. A comparison of gene expression between model group and control group indicated that there were 56 differentially expressed genes which included 32 up-regulated genes and 24 down-regulated genes. The known genes are shown in Table 3. Comparison of gene expression between therapy group and control group showed that there were only 11 differentially expressed genes, including 5 up-regulated genes (3 of them were also up-regulated genes in model group) and 6 down-regulated genes. Our data indicated that expression of 29 up-regulated genes and 24 down-regulated genes were modified by XQLD therapy and there was no difference when these genes expression were compared to their expression in control group.

A functional classification of the differentially expressed genes between model group and control group is shown in Figure 4. The number of differently expressed genes related to immune and inflammation responses is the largest except for not classified and functionally unclassified genes. Other differently expressed genes were involved in metabolism, gene expression, cell transportation, cell cycle, and cell proliferation.

4. Discussion

CS represents the most important environmental risk factors for respiratory diseases and it is the first risk for COPD (*12,13*). However, it needs a long time to establish rat COPD models with CS only. LPS is the major component of Gram-negative bacterium adventitia. It can damage airway epithelium directly, activate macrophages, lymphocytes, and neutrophils, induce bronchi chronic inflammation and cause emphysema formation. It stimulates secretion of specific pro-inflammatory molecules from circulating monocytes, such as IL-6 and monocyte chemotactic protein-1, and thereby aggravates progress of COPD (*14*). In this study, the COPD model was established by a modified method of combining fumigation and lipopolysaccharide (LPS) intra-tracheal dripping (*4*). Pathology appearances under a scanning electron

Table 3. Differentially expressed genes in model group when compared with control group

Gene name	Mean ratio	Function
Up-regulated genes		
Immunoglobulin joining chain	6.872	Immune
Fructose-bisphosphate aldolase A	4.708	Metabolism
Immunoglobulin heavy chain, α	4.556	Immune
Fertility related protein WMP1	3.884	Spermatogenesis
Norvegicus nucleoporin 62 (Nup62)	3.832	Gene expression
Immunoglobulin heavy chain 1a (serum IgG2a)	3.813	Immune
Chaperonin containing TCP1, subunit 5 (epsilon)	3.446	Cell transportation and cycle
Complement component 1, s subcomponent	2.967	Immune
CD36 molecule (thrombospondin receptor) (Cd36)	2.901	Signal transduction
Arginase, liver (Arg1)	2.727	Immune and inflammation
Sorting nexin 25 (Snx25)	2.533	Cell transportation and cell cycle
(α-*N*-acetyl-neuraminyl-2,3-β-galactosyl-1,3)-*N*-acetylgalactosaminide α-2,6-sialyltransferase 3 (St6galnac3)	2.519	Immune and inflammation
Leukotriene A4 hydrolase (Lta4h)	2.504	Immune and inflammation
Down-regulated genes		
6-Pyruvoyl-tetrahydropterin synthase (Pts)	0.371	Metabolism
3'-Phosphoadenosine 5'-phosphosulfate synthase 2 (Papss2)	0.353	Metabolism
Immunoglobulin superfamily, member 10 (Igsf10)	0.351	Immune
FK506 binding protein 9 (Fkbp9)	0.344	Immune and inflammation
Developmental arteries and neural crest EGF-like protein fibulin 5 (Fbln5)	0.343	Signal transduction
CEA-related cell adhesion molecule 1	0.341	Immune and inflammation
Acyl-coenzyme A oxidase 1, palmitoyl (Acox1)	0.340	Metabolism
Group specific component (Gc) vitamin D binding protein	0.330	Metabolism
Vitronectin (Vtn)	0.322	Cell migration and fibrosis
Neuronal PAS domain protein 2 (Npas2)	0.295	Gene expression
Phosphatidylinositol 3-kinase, catalytic, α polypeptide (Pik3ca)	0.244	Signal transduction
Eukaryotic translation initiation factor 2B, subunit 1 α	0.227	Gene expression

microscope and light microscope showed lesions in the rat model closely resemble COPD lesions occurring in humans.

Nutritional status disorders are the most common extra-pulmonary manifestations of COPD. A specific loss of weight, characterized by lean body mass (LBS), is observed in some COPD patients (*15*). In our study, animals in the model group and therapy group showed lower weight growth indexes than those in the control group ($p < 0.01$). Compared with the model group, the changes of general appearance, including LBS, in the therapy group demonstrated that XQLD was an effective drug which can relieve COPD symptoms.

Modern pharmacology studies have indicated that XQLD could down-regulate expression of γ-glutamylcysteine synthetase and nuclear factor-κB in bronchial and alveolar epithelium of COPD rats, which maybe responsible for gene expression regulation through multiple mechanisms. Our gene expression profiles analysis showed that the number of differently expressed genes between the model group and control group was 56 while there were only 11 differently expressed genes in the therapy group when compared to the control group. The genes involved were in immune and inflammation reactions, metabolism, cell transportation and cell cycle, signal transduction and gene regulation. Twenty-nine up-regulated genes and 24 down-regulated genes in the model group became non-differentially expressed genes after XQLD therapy. The changes of genes expression after XQLD treatment reflected that complicated genetic regulations were involved in the progression of COPD.

Differentially expressed genes related to immune response and inflammation mainly included *immunoglobulin heavy chain 1a* (*serum IgG2a*), *arginase 1*, alpha 2,6-*sialyltransferase*, *leukotriene A4 hydrolase*, *FK506 binding protein 9 (FKBP9)*, and *CEA-related cell adhesion molecule-1* (*CEACAM-1*). It is known that serum IgG2a (J chain) is a small polypeptide, which regulates polymer formation of immunoglobulin (Ig)A and IgM (*16*). Arginase-1 is an enzyme in arginine metabolism which plays an important role in asthma by decreasing nitric oxide production and increasing formation of peroxynitrite, polyamines and l-proline (*17*). Alpha 2,6-sialyltransferase is an acute-phase reactant and it is a Golgi membrane-bound enzyme (*18*). The leukotrienes are a family of lipid mediators involved in inflammation and allergy. Leukotriene B4 modulates immune responses, participates in the host defense against infections, and is a key mediator of PAF-induced lethal shock. The final step in the biosynthesis of leukotriene B4 is catalyzed by leukotriene A4 hydrolase, a unique bifunctional zinc metalloenzyme with an anion-dependent aminopeptidase activity (*19*). *Immunoglobulin heavy chain 1a* (*serum IgG2a*), *arginase 1*, alpha 2,6-*sialyltransferase* and *leukotriene A4 hydrolase* were up-regulated when COPD occurred. FK506 (tacrolimus), has powerful immunosuppressant properties and it can promote nerve regeneration (*20*).

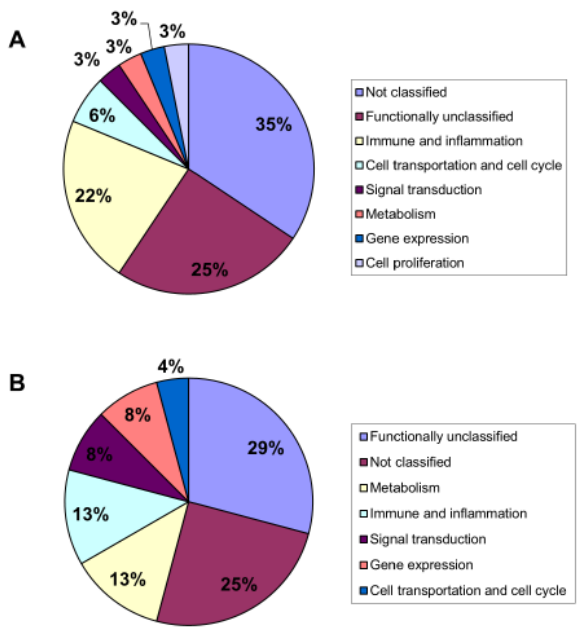

Figure 4. Functional classification of differentially expressed genes between model group and control group. **(A)** Functional classification of up-regulated genes between model group and control group. These genes were related to immune function and inflammation, cell transportation, cell cycle, signal transduction, metabolism, gene expression, and cell proliferation. **(B)** Functional classification of down-regulated genes between model group and control group. Most genes involved in metabolism, immune function and inflammation, signal transduction and gene expression.

FKBP9 encodes a protein related to FK506-binding protein 6 (65 kDa, FKBP65) which binds to FK506 (*21*) and plays an immunosuppression role. CEACAM1 appears to play a unique role among the neutrophil CEACAMs (*22*). Both *FKBP9* and *CEACAM1* genes were down-regulated in the model group compared to the control group.

There were also some differentially expressed genes related to gene expression regulation in the model group when compared to the control group. These genes included *nuclear pore protein p62* (*Nup62*), *neuronal PAS domain protein 2* (*NPAS2*) and the α-*subunit of eukaryotic initiation factor 2B* (*eIF-2B*). Transcription factor *Sp1* plays an important role in the expression of many cellular genes and it must interact with p62, through its C-terminus, to bring transcribeable DNA in contact with the transcription factors (*23*). In COPD rats, increased expression of p62 suggested up-regulated transcription of some genes. NPAS2 is a transcription factor expressed primarily in the mammalian forebrain (*24*) and it is an important transcription factor associated with circadian rhythms (*25*). Phosphorylation of eIF-2 is one of the best known mechanisms regulating protein synthesis in a wide range of eukaryotic cells, from yeast to human (*26*). In COPD rat models, *NPAS2* and *eIF-2* were negatively regulated but their roles in COPD are still unclear.

Some other differentially expressed genes between the model group and control group had a relationship with metabolism and signal transduction. *Fructose-bisphosphate aldolase A* (*Muscle-type aldolase*) involved in glycometabolism, was up-regulated while *6-pyruvoyl-tetrahydropterin synthase*, *3'-phosphoadenosine 5'-phosphosulfate synthetase 2* and *acyl-coA oxidase* were down-regulated. Differentially expressed genes associated with signal transduction included *epidermal growth factor* (*EGF*)-*related peptides* and *phosphatidylinositol 3-kinase catalytic subunit* α (*PIK3CA*). Both of these were down-regulated while their expression had no significant differencebetween the therapy group and control group. And also, there were some genes whose functions were not clear. They perhaps played a novel or important role in COPD genesis and development. Further study is still needed to explore these unknown genes.

5. Conclusion

Our results showed XQLD was an effective drug for COPD treatment and its function was related to gene expression alteration. A functional classification of differentially expressed genes indicated complex mechanisms involved in the genesis and development of COPD. Our results facilitate further investigation of the molecular mechanisms underlying the genesis and development of COPD and help us to understand mechanisms of XQLD in COPD therapy.

Acknowledgements

This study was supported by grant from Shandong science and technology program of China (No. 2002B17) and outstanding scholarship 1020 project of Shandong provincial health system.

References

1. Groneberg-Kloft B, Fischer A, Welte T. Fixed combination therapies in COPD – effect on quality of life. Int J Chron Obstruct Pulmon Dis. 2007; 2:551-557.
2. Siafakas NM. Preventing exacerbations of COPD – advice from Hippocrates. N Engl J Med. 2011; 365:753-754.
3. Miravitlles M, Soler-Cataluña JJ, Baranda F, Cordero P, Greses JV, de la Roza C. Previous outpatient antibiotic use in patients admitted to hospital for COPD exacerbations: Room for improvement. Infection. 2012; Epub ahead of print.
4. Zhang W, Zhang XY, Shao YM. Effects of TCM treatment according to syndrome differentiation on expressions of nuclear factor-κB and γ-glutamylcysteine synthetase in rats with chronic obstructive pulmonary disease of various syndrome types. Zhongguo Zhong Xi Yi Jie He Za Zhi. 2007; 27:426-430. (in Chinese)
5. Fang XM, Li J, Li ZG, Dong XB. Functional mechanism of pingchuanning decoction on adjustment of clara cell secretory protein in airway remodeling of asthmatic rats.

J Tradit Chin Med. 2012; 32:215-221.
6. Zhang CQ, Liang TJ, Zhang XY, Shao YM, He R, Zhang M, Long F, Li DW. Protective effect of Wenfei Huayin Recipe on lung of rats with chronic obstructive pulmonary diseases. Zhongguo Zhong Xi Yi Jie He Za Zhi. 2010; 30:72-75. (in Chinese)
7. Lesur I, Textoris J, Loriod B, Courbon C, Garcia S, Leone M, Nguyen C. Gene expression profiles characterize inflammation stages in the acute lung injury in mice. PLoS One. 2010; 5:e11485.
8. Nie YC, Wu H, Li PB, Luo YL, Zhang CC, Shen JG, Su WW. Characteristic comparison of three rat models induced by cigarette smoke or combined with LPS: To establish a suitable model for study of airway mucus hypersecretion in chronic obstructive pulmonary disease. Pulm Pharmacol Ther. 2012; 25:349-356.
9. Song YP, Cui DJ, Mao PY. A new way of establishing a rat chronic obstructive pulmonary disease model and the effects of drugs on them. Acad J PLA Postgrad Med Sch. 2001; 22:99-102. (in Chinese)
10. Sun GR, Xue WG, Gao B. Assessment on rat model of accumulation of cold and harmful fluid in lung with chronic obstructive pulmonary disease. World J Integr Tradit West Med. 2008; 3:635-639. (in Chinese)
11. Barbera JA, Peinado VI, Santos S, Ramirez J, Roca J, Rodriguez-Roisin R. Reduced expression of endothelial nitric oxide synthase in pulmonary arteries of smokers. Am J Respir Crit Care Med. 2001; 164:709-713.
12. Hill AT, Campbell EJ, Bayley DL, Hill SL, Stockley RA. Evidence for excessive bronchial inflammation during an acute exacerbation of chronic obstructive pulmonary disease in patients with α(1)-antitrypsin deficiency (PiZ). Am J Respir Crit Care Med. 1999; 160:1968-1975.
13. Mannino DM. COPD: Epidemiology, prevalence, morbidity and mortality, and disease heterogeneity. Chest. 2002; 121:121S-126S.
14. Aldonyte R, Jansson L, Piitulainen E, Janciauskiene S. Circulating monocytes from healthy individuals and COPD patients. Respir Res. 2003; 4:11.
15. Kuznar-Kaminska B, Batura-Gabryel H, Brajer B, Kaminski J. Analysis of nutritional status disorders in patients with chronic obstructive pulmonary disease. Pneumonol Alergol Pol. 2008; 76:327-333.
16. Johansen FE, Braathen R, Brandtzaeg P. Role of J chain in secretory immunoglobulin formation. Scand J Immunol. 2000; 52:240-248.
17. Maarsingh H, Zaagsma J, Meurs H. Arginine homeostasis in allergic asthma. Eur J Pharmacol. 2008; 585:375-384.
18. Jamieson JC, McCaffrey G, Harder PG. Sialyltransferase: a novel acute-phase reactant. Comp Biochem Physiol B. 1993; 105:29-33.
19. Haeggstrom JZ, Nordlund P, Thunnissen MM. Functional properties and molecular architecture of leukotriene A4 hydrolase, a pivotal catalyst of chemotactic leukotriene formation. ScientificWorldJournal. 2002; 2:1734-1749.
20. Chabas JF, Alluin O, Rao G, Garcia S, Lavaut MN, Legre R, Magalon G, Marqueste T, Feron F, Decherchi P. FK506 induces changes in muscle properties and promotes metabosensitive nerve fiber regeneration. J Neurotrauma. 2009; 26:97-108.
21. Jo D, Lyu MS, Cho EG, Park D, Kozak CA, Kim MG. Identification and genetic mapping of the mouse Fkbp9 gene encoding a new member of FK506-binding protein family. Mol Cells. 2001; 12:272-275.
22. Skubitz KM, Skubitz AP. Interdependency of CEACAM-1, -3, -6, and -8 induced human neutrophil adhesion to endothelial cells. J Transl Med. 2008; 6:78.
23. Han I, Roos MD, Kudlow JE. Interaction of the transcription factor Sp1 with the nuclear pore protein p62 requires the C-terminal domain of p62. J Cell Biochem. 1998; 68:50-61.
24. Reick M, Garcia JA, Dudley C, McKnight SL. NPAS2: An analog of clock operative in the mammalian forebrain. Science. 2001; 293:506-509.
25. Koudo R, Kurokawa H, Sato E, Igarashi J, Uchida T, Sagami I, Kitagawa T, Shimizu T. Spectroscopic characterization of the isolated heme-bound PAS-B domain of neuronal PAS domain protein 2 associated with circadian rhythms. Febs J. 2005; 272:4153-4162.
26. Alcazar A, Rivera J, Gomez-Calcerrada M, Munoz F, Salinas M, Fando JL. Changes in the phosphorylation of eukaryotic initiation factor 2 α, initiation factor 2B activity and translational rates in primary neuronal cultures under different physiological growing conditions. Brain Res Mol Brain Res. 1996; 38:101-108.

(*Received January 18, 2012; Revised September 3, 2012; Accepted October 18, 2012*)